

## Neoclassical Radial Current Balance in Tokamaks and Transition to the $H$ Mode

J. A. Heikkinen,<sup>1</sup> T. P. Kiviniemi,<sup>2</sup> and A. G. Peeters<sup>3</sup>

<sup>1</sup>VTT, Euratom-TEKES Association, FIN-02044 VTT, Espoo, Finland

<sup>2</sup>Helsinki University of Technology, Euratom-TEKES Association, FIN-02015 HUT, Espoo, Finland

<sup>3</sup>Max-Planck-Institut für Plasmaphysik-EURATOM Association, D-85748 Garching, Germany

(Received 26 May 1999)

Monte Carlo ion simulation based on neoclassical radial current balance in a divertor tokamak gives a stationary sheared  $\vec{E} \times \vec{B}$  flow. The neoclassical radial electric field  $E_r$  shows no bifurcation in contrast with earlier orbit loss models, but the shear in  $E_r$  reaches values at which a transition to enhanced confinement has been observed. Also, MHD turbulence analysis shows that a smooth transition can occur through the neoclassical  $\vec{E} \times \vec{B}$  flow shear suppression. The parameter scaling of threshold temperature for strong turbulence shear suppression agrees with the  $H$ -mode threshold scaling in ASDEX Upgrade.

PACS numbers: 52.25.Fi, 52.55.-s

Enhanced energy confinement is important in thermonuclear fusion since it can lead to an economically more attractive reactor. A transition from low confinement ( $L$  mode) to high confinement ( $H$  mode) is observed in many tokamaks and stellarators when the external heating of the plasma exceeds a threshold power [1,2]. Characteristic to the  $L$ - $H$  transition is the onset of a strong poloidal rotation of ions and rapid suppression of the fluctuation levels in the plasma edge at the transition [2,3] indicating the formation of a transport barrier, which at later times manifests itself through steep density and temperature profiles. It is the strong shear in the poloidal rotation, in particular, in  $\vec{E}_r \times \vec{B}$  flow [4], which is thought to result in the decorrelation of the turbulence [5] and, consequently, the strong reduction of anomalous energy transport. Here  $\vec{E}_r = E_r \hat{r}$  is the radial electric field and  $\vec{B}$  is the magnetic field. The source of the rotation is the key question in the theory of the transition.

Various explanations exist for the rapid growth in poloidal rotation speed  $v_\theta$ , its shear or curvature at the transition [2]. Orbit loss (OL) theory seeks for the balance of the outward nonambipolar orbit loss of particles and an inward neoclassical (NC) ion return current. In Ref. [6], multiple solutions of  $v_\theta$ , with a bifurcation in the rotation (and  $E_r$ ) when the collisionality  $\nu_i^* = \nu_{ii} R q / \nu_T \epsilon^{3/2}$  is around 1 in the plasma edge, are predicted. Here  $\nu_{ii}$  is the ion-ion collision frequency,  $\nu_T = (2k_B T / m_i)^{1/2}$  is the ion thermal velocity at the temperature  $T$ ,  $q$  is the safety factor,  $R$  is the major radius,  $\epsilon = r/R$ ,  $r$  is the radius, and  $m_i$  is the ion mass. In the experiment, however, the transition is often found for  $\nu_i^* \gg 1$  and at temperature that decreases with increasing ion density  $n$ , contradicting the  $\nu_i^*$  boundary for the transition. In other theories [7,8], the (turbulent) flows in the plasma edge are unstable to a well sheared  $\vec{E}_r \times \vec{B}$  flow. These theories of spontaneously excited spin-up in  $v_\theta$  need to specify how the driving terms continue to exist in the  $H$  mode. This question was addressed in Ref. [8] via a self-regulating shear flow turbulence with the turbulence energy, lost by  $E_r'$  damping, converted to rotation shear drive via the Reynolds stress.

The pressure gradient buildup by the barrier may also generate  $E_r$  in the stable  $H$  mode. Here the neoclassical  $E_r$  plays a role, although the transition parameters are not determined through NC effects in such a theory.

In this Letter, edge  $E_r$  dynamics and bifurcation from self-consistent fully kinetic 5D NC simulation of the tokamak edge with various plasma conditions are solved for the first time. By considering the orbit loss of both thermal and tail ions, the NC ion return current, and the ion distribution asymmetrization by losses and through redistribution by replacing ions (for charge neutrality), the main sources of the  $E_r$  shear are identified. The following results are discussed. First, there is no spontaneous bifurcation in  $E_r$  (even for  $\nu_i^* \leq 1$ ), i.e., no multiple solutions exist. The field changes smoothly, following the change in the plasma parameters. Second, with electrode polarization bifurcation in  $E_r$  is found and first numerical evidence of soliton structured  $E_r$  is observed. Third, although the Mach number  $M$  in the absence of polarization can be larger than one, this occurs only in a radially small region of a few mm, close to the separatrix and is sensitive to viscosity and the boundary conditions and unlikely is important in stabilization of turbulence. Fourth, although  $M$  is smaller than 1 over most of the domain, corresponding shear is still high enough for turbulence suppression within a wide enough radial region to a typical radial decorrelation length of the fluctuations. Fifth, high shear appears when the edge  $T$  becomes large. The effect of  $T$ ,  $n$ , toroidal magnetic field  $B_t$  (and its sign), plasma current  $I$ , and ion species on the shear is studied. Finally, a stringent constraint by orbit loss on fast transition is indicated.

Many different effects affect the evolution of  $E_r$  in the edge. First of all the ion orbits can have a width comparable to the gradient lengths in the edge leading to the breakdown of standard NC theory. A fraction of ions can escape over the separatrix and be lost on the wall or target plates, creating a nonambipolar flux that drives  $E_r$ , affected by gyroviscosity for large gradient of  $v_\theta$ . The field itself can in turn influence the orbits. Collisions populate the velocity loss cone but also prevent these ions from

completing their loss orbits and generate a return current through the viscous damping of (nonvanishing)  $v_\theta$ . The return and loss currents are strongly interlinked and are nonseparable. This complex interplay among several mechanisms requires a self-consistent computation. Here all these effects are included in evaluation of  $E_r$  from the Monte Carlo orbit following code ASCOT [9] applied for the divertor and limiter configurations [10,11].

In the code, the ion ensemble corresponding to the main plasma ions is initially distributed according to the assumed background  $n$  and  $T$  with Maxwellian energy distribution. Each ion is followed along its guiding-center orbit determined by the  $\vec{E} \times \vec{B}$ , gradient and curvature drifts, collisions, polarization, and viscosity drifts. The radial electric field  $\langle E_r(\rho, \theta) \rangle = -[d\Phi(\rho)/d\rho]\langle d\rho/dr \rangle$  on the magnetic surface with the coordinate  $\rho$  is evaluated from the condition  $\langle j_r \rangle = 0$  of the radial ion current density at all  $\rho$  and time  $t$ . Here  $\langle \dots \rangle$  denotes the flux surface (and ensemble) average and  $\theta$  is the poloidal angle. The  $E_r$  dynamics arises through the polarization drift  $v_{rp} = (1/\Omega B)\partial E_r/\partial t$  posed to each ion. Here  $\Omega = ZeB/m_i$  and  $Ze$  is the ion charge. Thus, the density profile  $\langle n(\rho, \theta) \rangle$  is automatically kept unchanged.

$E_r$  is solved with the NC ambipolar value  $E_a(r)$  [2] as an initial and inner boundary condition defined by zero parallel flow. At the inner boundary  $\rho = \rho_L$ , the outflowing particles are reflected by following without interactions their orbits outside, consistent with the assumption of no source of toroidal momentum and zero radial current. The outer boundary for the  $E_r$  evaluation is at the separatrix  $\rho = \rho_s$ . There  $E_r(\rho_s) = 0$  is adopted which pertains to the values of  $E_r$  for  $\rho > \rho_s$ , too. The ions are initialized within  $\rho_L < \rho < \rho_s$ , and those hitting the divertor plates or walls outside  $\rho > \rho_s$  are promptly reinitialized at the separatrix uniformly in pitch and poloidal angle with the local Maxwellian velocity distribution at  $\rho = \rho_s$ . This simulates well the replacement of the lost charge through the separatrix being more uniform in phase space than the loss process. It does not create unphysical current in the simulation domain and sustains any given  $n$  profile. As the ambipolar transport does not affect the current balance, the ion-electron collisions are neglected. As the collisions are evaluated with a fixed background for  $T(r)$  and  $n(r)$ , an energy source appears locally for the test ions to sustain the given  $T(r)$  profile in their ensemble. As  $\langle j_r \rangle = 0$ , there is no source of toroidal momentum and the parallel flow remains small. Thus, the corrections for momentum conservation [12] in collisions remain also small. To model high shear regions, perpendicular viscosity drift [13]  $v_{rv} = -(\eta/B^2)\partial^2 E_r/\partial \rho^2 |\nabla \rho|^2$  is included. Here  $\eta$  is the Braginskii viscosity coefficient [14], and the shear  $dv_\theta/d\rho$  has been approximated as  $(dE_r/d\rho)/B$ . Simulations with 300 000 ions in a 3 cm thick radial shell using 1/400 bounce time as time step for orbit tracking give a 150  $\mu\text{m}$  radial and 1  $\mu\text{s}$  time resolution in obtaining  $E_r$ . Each 2 ms run took about 12 h CPU time with a Digital Ev6 scalar processor.

Steady state is found by continuing the calculation for a sufficiently long time, typically several ms. Alternatively, steady state with  $dE_r/dt = 0$  has been sought for by directly iterating (with  $v_{rp} = 0$ ) the  $E_r$  profile until the given  $n$  profile for the ensemble is found. Both methods have resulted with the same steady state independent of the initial  $E_r$  profile indicating that the final state is stable and unique. In the steady state, the ions which have large orbit widths move out of the plasma and are lost on the divertor plates. The induced  $v_\theta$  (through  $E_r$ ) is not that of standard NC theory and the current of lost ions is balanced by a countercurrent of colder ions. Both the loss and return currents are driven by the ion-ion (-like particle) collisions. In practice, it has not been possible to radially resolve these currents separately.

For the ASDEX Upgrade configuration [10], the minor radius is  $a = 0.5$  m,  $R = 1.65$  m, elongation 1.6,  $I = 1$  MA, and  $B_t = -2.5$  T. Corresponding to shot No. 8044 for a deuterium plasma, a separatrix density  $1.2 \times 10^{19} \text{ m}^{-3}$  and temperature 120 eV with about 1.9 times larger values at  $r = a - 2$  cm are adopted for reference. Figure 1(a) shows the steady-state profiles of  $-d\Phi/d\rho$  in the region  $0.96 < \rho < 1$  ( $\rho_s = 1$ ) for various  $m_i$  and  $Z$  for the reference case but with  $4\times$  reference density.  $E_r$  on the outboard equator is found from  $d\rho/dr = 2 \text{ m}^{-1}$ .  $E_r$  is at an ambipolar level for  $|r - a| > 1-2$  cm with the Mach number  $M = |E_r/B_p v_T|$  of the rotation less than one. The decrease of  $E_r$  within  $|r - a| < 1$  cm is larger typically by an order of magnitude than the 1-2 kV/m decrease of the ambipolar value. Within a few mm from  $a$ , a deep well in  $E_r$  is found, where  $M$  can exceed 1. This narrow well should affect only weakly the turbulence over its radial decorrelation length  $\Delta r_t$  (about 1 cm). The so called Biglari-Diamond-Terry (BDT) criterion [5] for effective decorrelation is  $|dE_r/dr/B_t| > \Delta\omega_t/k_\theta \Delta r_t$ , where  $\Delta\omega_t$  is the decorrelation frequency and  $k_\theta$  is the mean poloidal wave number of the turbulence. Using typical values [15]  $\Delta\omega_t = 2\pi \times 40$  kHz,  $\Delta r_t = 0.7$  cm, and  $k_\theta = 1 \text{ cm}^{-1}$ ,  $\Delta\omega_t/k_\theta \Delta r_t$  becomes  $3.6 \times 10^5 \text{ s}^{-1}$ . Figure 1 shows that this criterion can be well satisfied in a wide enough region  $\geq \Delta r_t$ . Consistent with the ASDEX Upgrade experiments, deuterium gives higher shear (and lower  $H$ -mode threshold) than hydrogen. In the simulation, tritium gives the highest shear and helium the lowest.

Figures 1(b)-1(d) show  $-d\Phi/d\rho$  with deuterium for various separatrix  $n$ ,  $T$ , and  $B_t$  values scaled by a scalar multiplication of the reference profile. One finds that the BDT criterion is well met in a wide enough region  $\geq \Delta r_t$  if  $T$  is large. With  $n$  and  $B_t$  the shear increases only weakly. In a larger database, a somewhat weaker shear was found with the reversed  $B_t$ . The  $E_r$  profiles in Fig. 1 are well reminiscent of the measured  $E_r$  profiles at the transition in DIII-D [15] for the width or depth of the well. The profiles are robust to plasma parameters, and to the divertor configuration, as checked by modifying the position and number of the divertor plates. Effects of  $B_t$  ripple ion losses were weak. The obtained stationary states are the

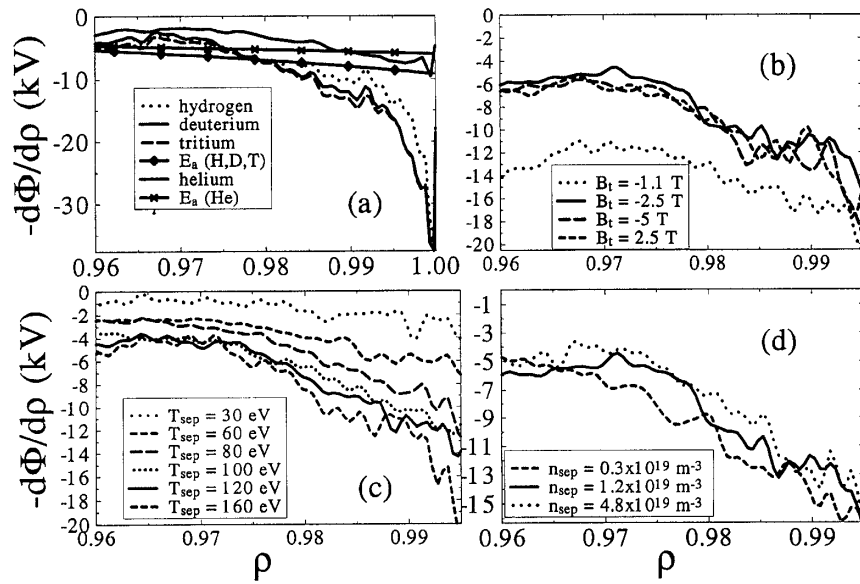


FIG. 1.  $-d\Phi/d\rho$  as a function of radius for various ion isotopes (a) in the reference case but  $n$  scaled by a factor of 4 up. Ambipolar values ( $E_a$ ) are also shown.  $-d\Phi/d\rho$  as a function of radius for various  $B_t$  (b), and separatrix  $T$  (c) and  $n$  (d). Other parameters are as for the reference case.

only solutions, and no bifurcation is found by changing parameters, even when  $\nu_i^*$  drops below 1.

Simulations were also performed for the biased experiments [11] where  $E_r$  is imposed externally by a polarization electrode in the edge and  $\langle j_r \rangle \neq 0$  in the plasma. Here the electrode current  $I_E$  and  $E_r$  profile were solved with the constraint of the given voltage between the electrode tip and limiter. In agreement with the TEXTOR experiments [11], bifurcation in  $I_E$  at a transition voltage  $U_{cr}$  was found. Interestingly,  $E_r$  profile bifurcated from a uniform shape to a solitary structure. Figure 2 shows the  $I_E$ -voltage curve and the soliton evolution for a 450 V voltage with the TEXTOR parameters [11] assuming no neutral damping. This gives the first numerical evidence for the solitary solutions suggested recently in Ref. [16]. The OL current was

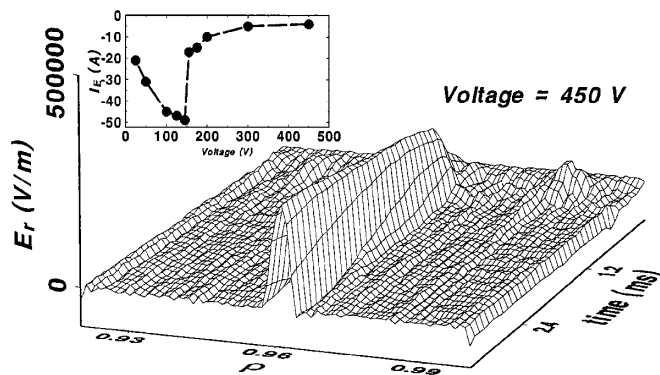


FIG. 2.  $E_r$  as a function of radius and time for 450 V polarization voltage starting with a uniform  $E_r$  radial profile.  $I_E$ -voltage curve is shown in the inset showing a transition at  $U_{cr} \sim 145$  V.  $n = 2 \times 10^{18} \text{ m}^{-3}$  and  $T = 40$  eV at  $r = a$ .  $I = 250$  kA,  $B_t = 2.35$  T,  $a = 0.46$  m, and  $R = 1.75$  m. Electrode tip-limiter distance is 4 cm.

here weak. The bifurcation and solitons appeared within  $\sim 2$  cm from  $a$  with  $U_{cr}$ ,  $I_E$ , position, width, and height dependent on  $\eta$ , viscosity, and neutral damping relevant for limiter tokamaks. Simulations thus support qualitatively the NC viscosity model as described in [6,11,17]. This was further confirmed by simulations of  $\nu_\theta$  relaxation rate with fixed  $E_r$  in the absence of OL. As fast transition is found with external current, but not spontaneously, self-consistency in treating radial current carriers appears crucial in a proper description of  $E_r$  dynamics.

Requiring  $(1/L) \int_{a-L}^a H(|\langle dE_r/dr \rangle|/B - 5 \times 10^5) dr > 0.7$  with  $L = 1$  cm that the shear exceeds a value  $5 \times 10^5 \text{ s}^{-1}$  at least within 0.7 cm just inside the separatrix, a temperature  $T_{cr}$  splitting shear in low and high values and its dependence on  $n$ ,  $B_t$ , and  $I$  are determined.  $H$  denotes the Heaviside function. In TEXTOR [11], critical shear for the  $H$ -mode was found to be  $|dE_r/dr| = 50\text{--}75 \text{ V/cm}^2$  at  $B_t = 2.35$  T, giving an experimental basis for the present choice of threshold independent of  $E_r$  generation. The weak variation of  $\langle dE_r/dr \rangle/B$  threshold in various tokamaks and the strong dependence of the shear on  $T$  as observed here justify the use of a fixed threshold to find the major scaling. In recent ASDEX Upgrade experiments, the critical temperature for the onset of the  $H$ -mode was found to scale as the function  $S(n, B_t, I) = 145n^{-0.3}|B_t|^{0.8}I^{0.5} \text{ eV}$  [18]. Here  $n$  and  $T$  have been evaluated at  $r = a - 2$  cm,  $T$  is expressed in eV,  $n$  in  $10^{19} \text{ m}^{-3}$ ,  $B_t$  in teslas, and  $I$  in mega-amperes. Figure 3 shows the shear rate from ASCOT for various  $T$  and the function  $S$ . A close agreement is found between the simulation and experiment. As a best fit to the shear in the numerical (deuterium) data one finds  $|\langle dE_r/dr \rangle|/B = 2964T^{1.06}n^{0.06}|B_t|^{-0.81}I^{-0.27} \text{ s}^{-1}$  with  $\pm 0.25$  error in exponents. The parameters were varied

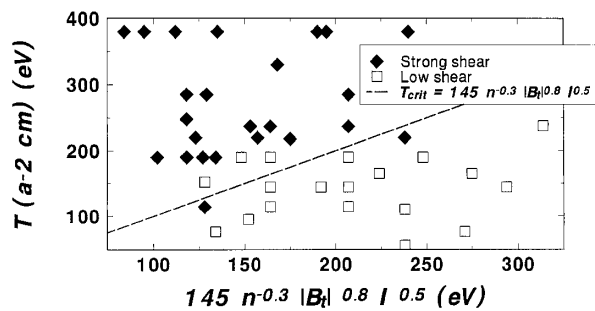


FIG. 3. Shear values of the  $\vec{E}_r \times \vec{B}$  flow as a function of the parametrization  $S = 145n^{-0.3}|B_t|^{0.8}I^{0.5}$  and temperature.

in the range  $B_t = -1.1$ – $(-5.0)$  T,  $I = 0.6$ – $1.5$  MA,  $n = 0.6$ – $12 \times 10^{19} \text{ m}^{-3}$ , and  $T = 30$ – $400$  eV, broader than in the experiments. Shear dependence on  $n$  and  $T$  was found to be stronger in the lower  $n$  and  $T$  data range, respectively. With the chosen threshold shear  $5 \times 10^5 \text{ s}^{-1}$ , one obtains  $T_{cr} = 126n^{-0.06}|B_t|^{0.76}I^{0.25} \text{ eV}$ .

As a paradigm for self-organized tokamak plasma edge turbulence, resistive drift wave equations [19] for the nonlinearly unstable vorticity, density, temperature, and parallel electron velocity fluctuations were solved by complementing them with an equation [20] for the evolution of the average poloidal  $\vec{E} \times \vec{B}$  flow velocity  $v_E$  in the presence of the electrostatic turbulent Reynolds stress and externally driven flow  $v(x, t)$ . Using our reference ASDEX Upgrade parameters with  $T = 100$  eV and  $n = 4 \times 10^{19} \text{ m}^{-3}$ , turbulence was followed for various shears  $V' = dv/dx$  with nonlinearly unstable initial amplitudes of turbulence. Figure 4 shows a nonlinearly saturated turbulence with a strongly suppressed level for largest  $V'$ . Suppression grows gradually with  $|V'|$  and becomes significant for  $|V'| \sim 5 \times 10^5 \text{ s}^{-1}$ . Turbulence suppression and perturbations in  $v_E$  by the Reynolds stress were weak and always dominated by the OL driven flow near the threshold conditions in Fig. 3. The results thus support the picture in Fig. 3 that the OL driven shear suppresses the turbulence and that this effect becomes pronounced around the transition threshold.

If the edge (ion)  $T$  grows slowly during external heating, only a slow transition can appear, if the shear reduces transport smoothly as in Fig. 4. Some tokamak experiments [15,21] see a weak  $E_r$  shear just before the transition and a fast suppression of turbulence and increase in shear at the transition on a time scale much shorter than changes in background  $T$ . In order to reconcile the present findings with them, a mechanism which can restrain the OL driven shear before and allow it just after a transition is required posing a new and strong constraint for any theory aiming to explain a *fast* transition. The theory has to be based on the evident presence of a strong OL drive of the shear. Any discrepancy of  $T_{cr}$  scaling between the experiments and present simulations may be explained by the parameter dependence of such an additional mechanism required, but as shown here for ASDEX Upgrade, such corrections

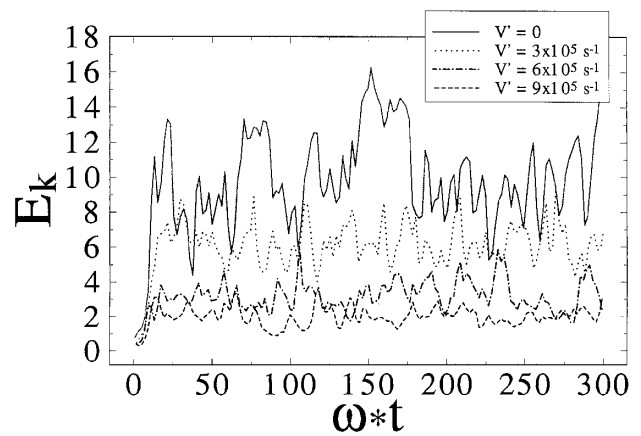


FIG. 4. Kinetic energy  $E_k$  in potential fluctuations (in arbitrary units) with various shears  $V'$ .  $\omega_*$  is the drift wave angular frequency.

may not be dominant with major scaling arising from the OL driven shear.

This work benefited from the computing resources of the Centre of Scientific Computing in Espoo, Finland.

- 
- [1] F. Wagner *et al.*, Phys. Rev. Lett. **49**, 1408 (1982).
  - [2] K. Itoh and S.-I. Itoh, Plasma Phys. Controlled Fusion **38**, 1 (1996), and references therein.
  - [3] K. H. Burrell *et al.*, Phys. Fluids B **2**, 1405 (1990).
  - [4] Y. B. Kim *et al.*, Phys. Fluids B **3**, 384 (1991).
  - [5] H. Biglari, P. H. Diamond, and P. W. Terry, Phys. Fluids B **2**, 1 (1990).
  - [6] K. C. Shaing and E. C. Crume, Jr., Phys. Rev. Lett. **63**, 2369 (1989).
  - [7] A. B. Hassam *et al.*, Phys. Rev. Lett. **66**, 309 (1991).
  - [8] P. H. Diamond *et al.*, Phys. Rev. Lett. **72**, 2565 (1994).
  - [9] J. A. Heikkinen and S. K. Sipilä, Phys. Plasmas **2**, 3724 (1995).
  - [10] V. Mertens *et al.*, in *Proceedings of the 20th European Conference on Controlled Fusion and Plasma Physics, Lisbon* (European Physical Society, Petit-Lancy, Switzerland, 1993), Vol. 17C, Part I, p. 267.
  - [11] R. R. Weynants *et al.*, Nucl. Fusion **32**, 837 (1992).
  - [12] X. Q. Xu and M. N. Rosenbluth, Phys. Fluids B **3**, 627 (1991).
  - [13] L. Spitzer, *Physics of Fully Ionized Gases* (Interscience Publishers, New York, 1962), 2nd ed., Eq. (2.42).
  - [14] S. I. Braginskii, *Reviews of Plasma Physics* (Consultants Bureau, New York, 1965), Vol. 1.
  - [15] P. Gohil, K. H. Burrell, and T. N. Carlstrom, Nucl. Fusion **38**, 93 (1998).
  - [16] K. Itoh *et al.*, Phys. Plasmas **5**, 4121 (1998).
  - [17] T. Stringer, Nucl. Fusion **33**, 1249 (1993).
  - [18] W. Suttrop *et al.*, Plasma Phys. Controlled Fusion **39**, 2051 (1997).
  - [19] B. D. Scott, Phys. Fluids B **4**, 2468 (1992).
  - [20] H. Sugama and W. Horton, Phys. Plasmas **1**, 345 (1994).
  - [21] R. A. Moyer *et al.*, Phys. Plasmas **2**, 2397 (1995).